Characterization and Evaluation of Cordless Nailer Performance for Liquid and Gaseous Fuels

Mark Carioscio
Marquette University

CHARACTERIZATION AND EVALUATION OF CORDLESS NAILER PERFORMANCE FOR LIQUID AND GASEOUS FUELS

by

Mark J. Carioscio, B.S.M.E.

A Thesis submitted to the Faculty of the Graduate School,
Marquette University,
in Partial Fulfillment of the Requirements for
the Degree of Master of Science

Milwaukee, Wisconsin

December 2018

ABSTRACT
CHARACTERIZATION AND EVALUATION OF TOOL PERFORMANCE FOR LIQUID AND GASEOUS FUELS FOR A CORDLESS NAILER

Mark J. Carioscio, B.S.M.E.

Marquette University, 2018

The Paslode Cordless XP Framing Nailer is a combustion-powered nail gun that operates using a fuel blend of a propylene and 1-butene. This tool is designed to drive nails using a piston driven by a combustion reaction. The current fuel blend is able to fire approximately 1200 shots per fuel cartridge and match the energy output of pneumatic, corded nailers on the market. This thesis is written with the intent to gain a better understanding of the operation of the tool and how its performance varies when the fuel source is altered.

A bizonal combustion model was created to simulate the operation of the tool. The model predicts the unburned gas temperature, burned gas temperature, piston displacement, compression pressure due to the rapid travel of the piston, and combustion pressure. The model predicts the importance of two key factors when selecting a fuel – the laminar flame speed and the energy density of the fuel. To validate the model, an experimental test stand and redesigned combustion chamber were developed. The test stand provided clean, repeatable results for both liquid and gaseous fuels. The fuels tested were 1-butene (gas), propane (gas), propyne (gas), heptane (liquid), and iso-octane (liquid). The current fuel blend was used as a benchmark to compare the fuels.

The fuels that performed best, using the metric of boundary work done on the piston, were those that had higher lower heating values. However, the fuels with higher energy density provided more volumetric efficiency. Flame speed was shown to positively affect the peak chamber pressure but should be considered as a secondary metric for optimizing tool performance. This thesis characterizes the performance of the tool using several fuels. Based on these results, an ideal fuel for the XP Framing Nailer would be a fuel blend that would have a high volumetric energy density.

ACKNOWLEDGEMENTS

Mark J. Carioscio, B.S.M.E.

I would like to first thank my advisor, Dr. Casey Allen. Without your endless guidance and support over the past four years, there is no chance I would be where I am today. You inspired me as an undergrad and convinced me to pursue another degree. On top of the actual thermodynamics and combustion lessons, you taught me the importance of a strong work ethic to achieve the goals set in front of me. I could not have asked for a better mentor and role model.

I would also like to thank my fellow T_{ad}poles. Jack and Jenna, you welcomed me into the lab with open arms and helped me learn what it takes to be successful as a grad student. You warned me of challenges but also showed me how to enjoy my time in the lab. Ashley, David R., and Dylan, you all pushed me to achieve and supported me down the final stretch. And David W., you were constant throughout my time in grad school – always there to help, listen, or motivate. You all rock and I would not be here without you!

To my thesis committee of Dr. Singer and Dr. Roy: thank you for being great teachers as well as supporting me on my committee. I appreciate the critical feedback and thank you for making my thesis better.

Thank you to my girlfriend, Taylor. Through the highs and the lows of this entire process, you've been there for me. You've listened to me complain about the workload and you've been excited when I had breakthroughs (no matter how small). I love you and I'm excited to start the next chapter of our lives together.

Lastly, I'd like to thank my family. They are a constant in my life – always supporting and always loving me. I cannot stress enough how much I notice and appreciate the unconditional love and guidance I get from you all. Thank you!

Contents

List of Tables

Table of Figures

Chapter 1. Introduction

The Paslode tool manufacturing division of Illinois Tool Works (ITW) developed a tool designed to utilize the power of combustion to rapidly drive nails into a surface. The tool, now known as the XP Cordless Framing Nailer, is a complex machine that has gone through many fuel changes over the past decade. The tool performance has varied with different fuels and thus arose a question regarding optimization: what fuel or fuel blend will provide the best tool performance? This question is the driving force behind this thesis.

The question is addressed from two angles. First, a physics-based combustion model written in Python is designed to gain better understanding of the tool. The model represents a simplified system of how the tool functions, but it comes with many sub-models that require validation. Second, experiments were performed with the tool to test how different fuels perform and to validate the model. Paired together, the model guided the fuel selection for the experiments which, in turn, helped to validate the model.

This thesis evaluates the tool performance of four gaseous fuels and two liquid fuels to gain more knowledge towards solving the overall goals put forward by ITW. These goals are to obtain more powerful shots and more shots per cartridge while holding the form factor of the cartridge constant.

1.1 Outline

The thesis begins with a background section consisting of two parts. It initially discusses the Paslode Cordless XP Framing Nailesr and how it operates. Then, other nailers are presented and their function is described. After that, the paper reviews advantages and disadvantages of the current combustion design and discusses the current fuel blend.

Chapter 3 further describes how the tool is modeled. It begins with modeling background. Then, it introduces the system of differential equations that must be solved to predict tool behavior. It elucidates the sub-models that are not combustion-related. These sub-models are required to understand the impact of combustion and quantify the success of a trial. It introduces a bizonal model for combustion consisting of an unburned and burned gas zone. Unburned gas zone is converted into the burned gas zones as the flame travels through the chamber. It finally discusses the mass burn rate with respect to the bizonal model and how the flame propagates.

Chapter 4 discusses the methodology behind the experimental portion of the thesis. It opens by explaining the test stand designed specifically for the XP nailer. It then describes the combustion chamber designed to accommodate high-speed camera video required to measure flame propagation. Next, the fuel options and how they are tested are described in detail.

Chapter 5 contains the results of the experimental testing. It starts by showing results from both versions of the test stand. It then discusses the different metric options for evaluating tool performance. The two main metrics investigated are peak pressure and boundary work done on the piston. The thesis then focuses on the boundary work done on the piston and investigates these results. The possibility of blending candidate fuels is also discussed. Finally, the experimental results are compared with the model predictions. High speed video of flame propagation is also shown here to show how the experiments can influence model parameters.

Chapter 6 is the final section. It is a summary of the thesis and includes a section describing what should be done in the future to continue this project. The future work portion has two sections: future modeling work and future experimental work.

Chapter 2. Background

2.1 Paslode Cordless XP Framing Nailer

The Paslode Cordless XP Framing Nailer is a unique tool in the framing nailer market because it utilizes combustion to drive nails. Most nailers on the market are pneumatic tools which require an air hose and air compressor. Pneumatic tools fire nails by applying pressure to the piston head – when the trigger is fired, the high-pressure air is routed such that it forces the piston to drive the nail. The tools that do not rely on pneumatics are called “cordless”. There are three main designs of cordless nailers that can be seen on the market: spring-loaded, electromagnetic, and combustion. The spring-loaded design uses springs actuated by a battery-powered motor to generate the hammering force. The electromagnetic design uses a battery to power a solenoid containing a magnetic piston. Running current through the solenoid creates a magnetic field which forces the piston to move and drives the nail (Harris, n.d.). The final cordless nailer design uses a single stroke combustion chamber to drive the nail. A sealed combustion chamber is dosed and sparked generating an increase in pressure. The pressure increase pushes the piston down the cylinder and drives the nail into the surface. Within the cordless framing nailer market, the XP is currently the only tool that is powered by the combustion design.

The XP Framing Nailer is lightweight compared to other nailers on the market. Its main advantage is that it is a cordless nailer that can produce a similar amount of power to

the corded, pneumatic alternatives (Mahoney, 2010). Battery-powered cordless nailers cannot generate the same power and performance provided by the pneumatic nailers. The XP nailer uses a battery but the power generation comes from the fuel cartridge. The fuel cartridge is a cylinder with two compartments inside of it. The first part is a bag connected to the port which holds the fuel. The second part of the fuel cartridge is the volume surrounding this bag. The second compartment is filled with aerosol to pressurize the bag so that the fuel is in liquid form. This nailer can match the power of the pneumatic tools because of its combustion design. Another advantage it has is that, while it is as powerful as pneumatic nailers, the recoil, or kickback of the tool when firing, is relatively small (Koehler, 2018).

The advantage created by the fuel cartridge design comes packaged with a disadvantage – the tool requires a cartridge to provide fuel as well as a battery to spark the chamber. A tool without both will not be operable, but other cordless nailers require only batteries to operate. A second disadvantage that comes with the current tool is the inability to be used with a "bump-fire" mode. Ease of use is essential for any tool and a common practice with nail guns is to hold the trigger down and rapidly tap the tool's safety mechanism against the wood to hammer nails, commonly referred to as "bump-firing" (Safety Alert - Safe Use of Nail Guns, 2012). The combustion design of the XP requires the trigger to be pulled each time a nail is to be fired. This is because the trigger provides the energy to spark the chamber, igniting the fuel-air mixture to create the pressure rise. Attempting to bump-fire the XP will cause the chamber to dose with fuel for each "bump" and never fire. It will not fire after each bump because pulling the trigger will spark the chamber – no spark leads to no ignition. The third and final disadvantage associated with

combustion is the exhaust – the odor can be unappealing and unburned fuel can be dangerous to consumers. Incomplete combustion and fuel-rich conditions can cause consumers to inhale hydrocarbons which have not been fully broken into water and carbon dioxide. Not only is this unhealthy for consumers, but it has a negative impact on the environment.

Figure 1. Paslode XP Framing Nailer (Paslode's New CF325XP & PF250S-PP Nailers, 2015)

This thesis focuses on the Paslode XP Framing Nailer, seen in Figure 1. The tool uses a single shot combustion chamber to drive a nail. As the chamber is closed, a mechanical link presses on the top of the fuel cartridge releasing fuel. The current fuel is 70% propylene (propene) and 30% 1-butene on a molar basis. The fuel cartridge releases somewhere between 23 and 27 mg of fuel each time the chamber closes. While the chamber is closing, a switch engages a fan inside of the combustion chamber. The fan serves three

main purposes: to mix the fuel and the air inside of the chamber before combustion, to enhance flame propagation during combustion, and to aid in venting the exhaust gases after combustion. Once the fuel is dosed (injected into the combustion chamber), the fan mixes the contents of the chamber and the tool is ready to fire. The trigger can be pulled, causing the spark plug to release enough energy to ignite the mixture. The pressure inside of the chamber rises and forces the piston to move down the piston cylinder. The piston strikes the nail with enough momentum to break the nail from the strip of nails and drive it into the surface. The piston returns to "top dead center" due to a build-up of compressed air as well as a bumper which acts as a spring. Additionally, the fan also cools the exhaust gases which creates a small vacuum aiding in the return of the piston. The chamber opens once the tool is removed from the surface. When the chamber opens, the fan blows out the exhaust gas which is replaced by air from the surroundings. As the tool is pressed onto the surface again, the process repeats.

The tool currently uses a blend of propylene and 1-butene. These two hydrocarbons are gases in standard state. The tool can also be fired with other fuels and other blends of fuels, but performance can vary with a change in fuel. The tool was originally fired with MAPP gas which is a blend of propyne (48%), propane (27%), and propadiene (25%). When the composition of MAPP gas was changed, propylene and butane were added to the mixture (MAPP Gas, 2018). The mixture became 30% propyne, 14% propadiene, 43% propylene, 7% propane, and 6% butane. This change caused a decrease in performance which in turn caused Paslode to change the fuel used for the tool. Initially, ITW fired with a 50-50% molar blend of propylene and 1-butene before settling on the 70-30% molar

blend they use today. All the fuels used on this tool are hydrocarbons. Hydrocarbon fuels are very useful because they are highly energy dense.

Chapter 3. Model

3.1 Modeling Background

Modeling the behavior of the tool requires a strong understanding of the forces working on the piston. The driving force in the tool is the increase in chamber pressure due to combustion in the chamber. This can be modeled using a multi-zone method. The chamber can be broken up into zones of unburned gas, reacting gas, and burned gas. As the flame front (reacting gas) propagates through the chamber, the unburned gas is converted into burned gas and energy is released. Each zone is analyzed using an energy balance to calculate temperature (Christian Foin, 1999). Temperature rises due to the heat released from the combustion reactions:

Equation 1. Combustion Reaction

$$Fuel + Oxidizer \rightarrow Product + Energy$$

Temperature decreases through the heat loss in the walls. The increase in energy/temperature corresponds to an increase in pressure and eventually volume according to the ideal gas law:

Equation 2. Ideal Gas Law

$$PV = nR_uT$$

Where P is the pressure, V is the volume, n is the number of moles in the closed system, R_u is the universal gas constant, and T is temperature. As heat is released into the chamber, the temperature rises, and the pressure rises to balance the equation. Once the pressure rises enough to overcome the static friction between the piston and cylinder walls, the volume also begins to increase as energy is released. The amount of energy released and the rate at which it is released is determined by the fuel and the stoichiometry of the mixture.

A unique component of this combustion chamber is the spinning fan. While it makes modeling easier because it can be assumed that the chamber is a well-stirred reactor (Turns, 2012), it also creates a highly turbulent flame propagation. Laminar flames can be modeled as a spherical kernel of flame propagating radially (Sokratis Demesoukas, 2013). This flame sphere propagates at a rate called the laminar flame speed (S_l). This rate is defined at the propagation of a one-dimensional, planar, adiabatic premixed flame at a given temperature, pressure, and stoichiometry (S. G. Davis, 1998). This would provide a straightforward calculation of how quickly the unburned gas is converted into burned gas and therefore how quickly the energy is released. However, the turbulence added by the fan creates a need to model premixed turbulent combustion. There are several numerical methods for modeling the stochastic nature of turbulence. Direct numerical simulation (DNS) is a method which involves solving the entire set of governing equations. DNS has a very high computational cost, so some models use the Reynolds averaged Navier-Stokes (RANS) method. RANS modeling assumes the turbulent flame is a random process and then solves for the statistical mean field. RANS is computationally cheap compared to most methods. Another way to model turbulent combustion is via large eddy simulations (LES). LES focuses the modeling on the large-scale wrinkling. This is computationally cheaper

than DNS but more expensive than RANS. However, for this project, it was deemed too difficult to determine the validity of these combustion sub-models and therefore a simpler method was used to approximate the combustion reactions and turbulent nature of the flow.

A simpler method is simulation of the flame surface area as a hemisphere which propagates in a laminar fashion. The equation for mass burn rate can be written as:

Equation 3. Mass burn rate from Grill

$$\frac{dx_b}{dt} = \frac{\rho_u A_{flame} S_l}{m_{total}}$$

Where x_b is the mass burn fraction, ρ_u is the density of unburned gas, A_{flame} is the flame surface area, S_l is the laminar flame speed, and m_{total} is the total mass of the system (M. Grill, 2006). If the flame surface is assumed to be wrinkled (a rough surface with bumps rather than smooth), a greater surface area will cause the mass to burn at a faster rate. Additionally, a greater flame speed will provide the same effect.

Flame speed is the rate at which the reaction (flame) front propagates. It is a measure of how an observer riding with the flame would experience the approach of the unburned flame (Turns, 2012). To determine the flame speeds of various fuels, a script was developed in Python which utilizes Cantera. Cantera is an open source computing tool that allows users to evaluate thermodynamic and chemical kinetic reactions (About Cantera, 2018). Cantera allows users to calculate flame speeds given a fuel-air mixture, a set of conditions, and a series of chemical reactions. A series of chemical reactions is also known as a kinetic mechanism. Given the fuel and the conditions, Cantera simulates combustion using one of these kinetic mechanisms. The accuracy of the predictions made by Cantera is based directly on the accuracy of the kinetic mechanism. A complex fuel requires a

detailed kinetic mechanism for Cantera to produce accurate combustion results (including flame speed). Cantera produces a laminar flame speed given a set of conditions and given a chemical kinetic mechanism.

Another factor of importance is the heating value of the fuel. There are two types of heating values, higher and lower. The heating value is the amount of thermal energy released during combustion. The higher heating value is calculated by determining the enthalpy (total heat content of a system) of the products at pre-combustion conditions and with water treated as a liquid. The lower heating value, or LHV, is the same calculation but treats any water formed as a vapor (which has a lower enthalpy). LHV is a factor that is considered for all fuels selected in this thesis.

3.2 Tool Modeling

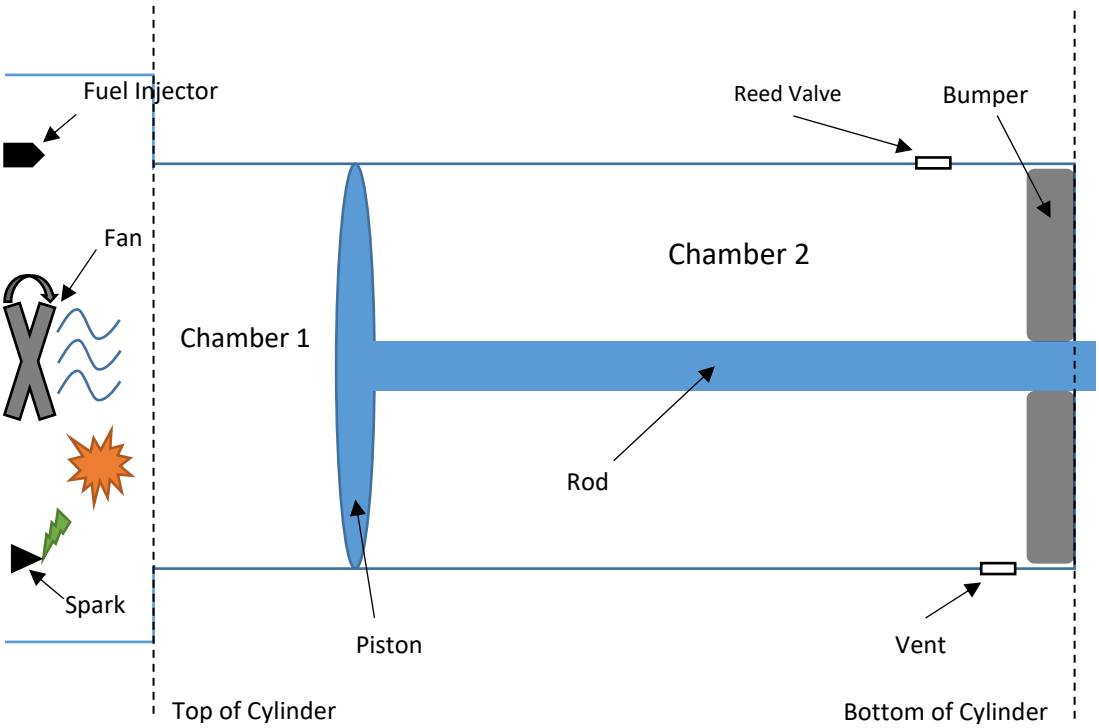

Figure 2. Nomenclature of inside of tool for modeling

The cordless nailer model, shown in Figure 2, simulates the position of the piston as a function of time from a coupled set of ordinary differential equations (ODEs). The core of the model is based on a force balance applied to the piston as follows:

Equation 4. Force balance on piston

$$P_1 A_1 - P_2 A_2 - F_{fr} = m\ddot{x} + b\dot{x} + kx$$

- P_1: Pressure in chamber 1 (*i.e.*, driving pressure side)
- A_1: Piston surface area in chamber 1
- P_2: Pressure in chamber 2 (*i.e.*, vent side)
- A_2: Piston surface area in chamber 2
- F_{fr}: Frictional force
- m: Piston mass
- x: Piston position, dot ($\dot{x}$) represents derivative with respect to time
- b: Bumper damping coefficient ($b = 0$ during non-contact)
- k: Spring constant ($k = 0$ during non-contact)

This model can be integrated to yield the piston position as a function of time. To make the model functional, additional physics within the tool must be simulated. For example, to determine the pressure in Chamber 1 used in the force balance, an open system energy balance must be used with a combustion model and valve flow model. The following sub-models are used to represent these physics:

Table 1. Sub-models and their descriptions

Sub-Model	**Description**
Energy Balance	Open system energy balance with ideal gas assumption (for both chambers 1 and 2).
Combustion Model	Mass burn rate dictating energy release
Mass Flow	Compressible flow through the valves

Tracking the location of the piston is important to understand the tool behavior. In Equation 5 (below), the rate of change of displacement (x) is calculated with velocity (v):

Equation 5. Displacement

$$\frac{dx}{dt} = v$$

To determine the change in velocity with respect to time, the forces acting on the piston are considered. In Equation 6, the damping constant (b) and spring constant (k) are used as tuning parameters. The change in pressure (ΔP) acting over the surface area of the piston (A) is the factor that drives the model. The mass of the piston is denoted by "m".

Equation 6. Velocity

$$\frac{dv}{dt} = \frac{-bv - kx + \Delta PA}{m}$$

The rate of pressure change is determined using the first law of thermodynamics. This can be seen in Equation 7. The fuel heat capacity ratio (k) over the volume of the combustion chamber is multiplied by the energy released from the fuel (Q). This energy is released at the rate of fuel being burned (x_b). The change in volume with respect to time is multiplied by the heat capacity ratio and pressure over the volume.

Equation 7. Pressure

$$\frac{dP}{dt} = \frac{(k-1)}{V} * Q\frac{dx_b}{dt} - \frac{kP}{V}\frac{dV}{dt}$$

The rate of volume change with respect to time is seen in Equation 8. It is determined by the radius of the piston squared times pi and the velocity.

Equation 8. Volume

$$\frac{dV}{dt} = \pi r^2 v$$

The unburned gas volume is determined by determining the decrease in unburned volume due to the flame propagation. Additionally, the unburned gas volume is also a function of the change in pressure with respect to time.

Equation 9. Unburned gas volume

$$\frac{dV_u}{dt} = -V_u \left(\frac{m_{tot}}{N_u M_u} \frac{dx_b}{dt} + \frac{1}{kP} \frac{dP}{dt} \right)$$

The number of moles of unburned gas and burned gas in the chamber (Equations 10 and 11) are determined using the mass burn fraction $(\boldsymbol{x_b})$**.** These are not differential equations and are therefore calculated after the simulation is performed. These are important variables for determining the combustion performance.

Equation 10. Number of moles of unburned gas

$$N_u = \frac{m_{tot}}{M_u}(1 - x_b)$$

Equation 11. Number of moles of burned gas

$$N_b = \frac{m_{tot}}{M_b}(x_b)$$

The temperature of the burned gas (T_b) is calculated using the Ideal Gas Law, seen in Equation 12. This equation is also not a differential equation and therefore, the burned gas temperature is calculated after the simulation is run. N_b is the number of moles of burned gas and $\bar{R}$ is the universal gas constant.

Equation 12. Temperature of burned gas

$$T_b = \frac{P(V - V_u)}{N_b \bar{R}}$$

The unburned gas temperature (T_u) is calculated assuming the unburned gas is initially uniform and undergoes isentropic compression (Heywood, 1988). Equation 13 shows how this is calculated. T_o and P_o are initial temperature and initial pressure respectively.

Equation 13. Temperature of unburned gas

$$\frac{dT_u}{dt} = \frac{T_o}{P_o}\left(1 - \frac{1}{k_u}\right)\left(\frac{P}{P_o}\right)^{-\frac{1}{k_u}}\frac{dP}{dt}$$

These equations were made to simulate the tool performance. The focus of this project is the combustion aspect of the tool so although the dynamics are important, the most significant equation is the equation for pressure (Equation 7). The first term in the equation describes energy released into the system (Q) which is based on fuel properties. Additionally, the rate at which this energy is released ($\frac{dx_b}{dt}$) is essential to the tool performance. The next section will discuss how this is modeled.

3.3 Combustion Modeling

The combustion portion of the model is described by the energy release due to the combustion according to the mass burn rate of the fuel. The total energy released is calculated using the fuel properties and the mass burn rate is calculated by approximating the propagation of the flame within the cylinder:

Equation 14. Mass burn rate

$$\frac{dx_b}{dt} = \frac{\rho_u Y_u S_t A_f}{m_{tot}}$$

- x_b: Fuel mass burn fraction
- p_u: Density of the air/fuel mixture in the unburned region
- Y_u: Fuel mass fraction in the unburned region
- S_t: Turbulent flame speed
- A_f: Surface area of the flame (curve-fit function based on geometry)
- m_{tot}: Total mass inside combustion chamber

The fuel mass burn fraction is a measure of how much mass in the chamber has been converted into exhaust. If no mass has been consumed, the mass burn fraction will be 0. If all the mass is consumed, the mass burn fraction will be 1. As previously described, the inclusion of laminar flame speed in this equation provides the essential link to modeling the influence of fuel combustion properties on tool performance. During the first month of this project, flame speeds were investigated for varying fuels, which revealed that minor composition changes can substantially influence flame speed (e.g., 10% molar doping of acetylene into methane increased flame speed by 25%). However, laminar flame speed is not as important as how each fuel burns with respect to the turbulence caused by the fan.

Another key component in the current model is the inclusion of a caloric equation of state which relates energy to temperature. This improvement allows gas temperature (both burned/unburned) to be calculated so that accurate predictions for heat loss can be made.

Before the bizonal model was developed, the mass fraction burned profile was arbitrarily specified by a Wiebe function. A Wiebe function is a combustion model that can

be modified to match data. Because the goal of the model was to be predictive, a new combustion model was developed. The current model calculates the mass fraction burned by initializing a flame kernel with a small volume, generated by a spark. The current model has a spark radius of 0.01cm initially – this value was determined by fitting model results to experimental data. Changing this radius affects the burn rate and tool performance. This number was selected because it produced the best agreement with validation. The flame propagates radially converting unburned gas to burned gas according to a "volumetric flowrate" that is calculated as $\dot{V} = A_f S_t$. This equation shows that both the turbulent flame speed and the flame surface area are important factors for predicting the mass fraction burn rate. The turbulent flame speed is calculated as an arbitrarily chosen tuning parameter, known as wrinkling factor, multiplied by the laminar flame speed:

Equation 15. Turbulent Flame Speed

$$S_t = \Xi S_l$$

The flame surface area calculations assume a hemisphere with radius *r* propagates at a rate determined by the flame speed. Figure 3 shows an example of the bizonal model results. Figure 3a shows the burned and unburned volumes and Figure 3b shows the mass burn rate. The growth of the hemisphere is limited, however, due to the geometry of the combustion chamber. Any portion of the flame surface area that contacts the combustion chamber walls or piston is ignored. This is evident in Figure 3c at a time of t = 0.027 s. Just prior to this time, the flame surface area is roughly equal to the piston surface area but is suddenly reduced to A_f = 0 when the flame impinges on the piston. The plot in 3c also shows flame surface area as non-zero when the mass fraction burned is equal

to 1, but this is not possible in practice. From a modeling standpoint, the flame surface area is based simply on the geometry of Chamber 1. This is a curve-fit modeling parameter that the model calls to calculate mass burn rate. Once the mass burn fraction reaches 1, mass burn rate goes to zero and the flame surface area (based solely on geometry) does not affect the results. This radially propagating flame is a simple foundation to begin with but is likely inaccurate. Further flame visualization experiments could reveal how the fan influences the true flame shape so that model improvements can be made.

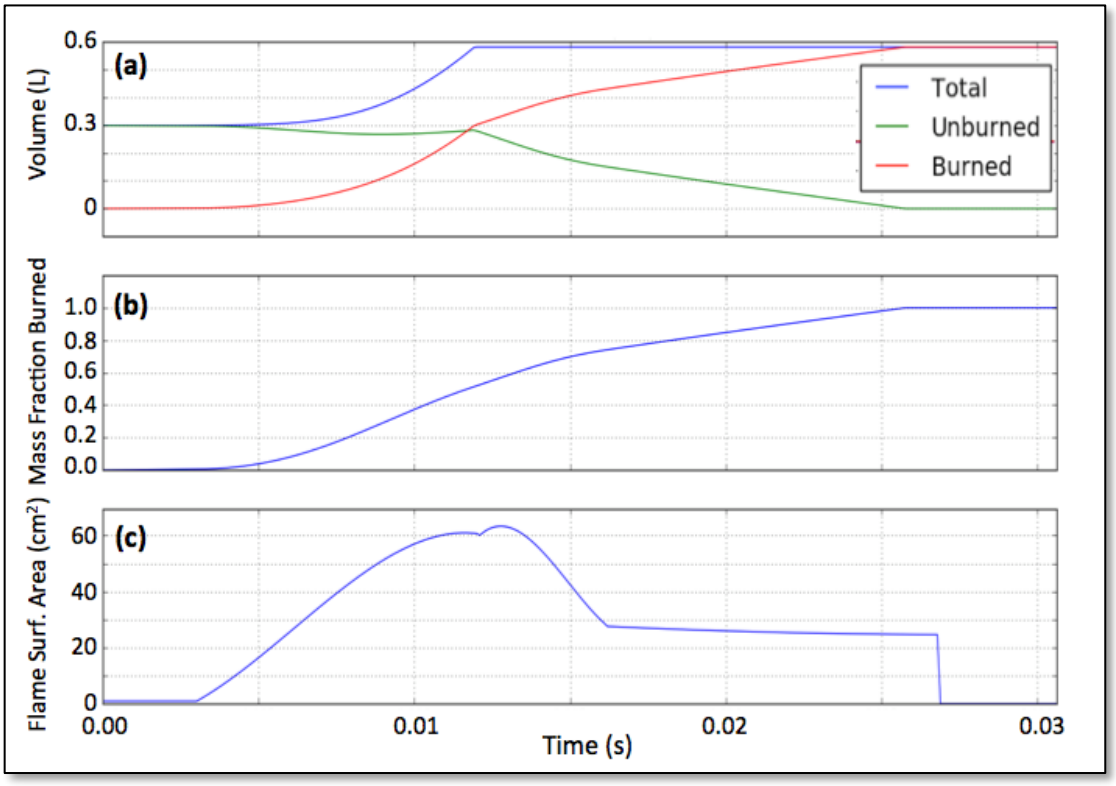

Figure 3. Model predictions of volume, mass burned fraction, and flame surface area

Chapter 4. Methodology

4.1 Test Stand

Two unique test stands were designed to collect data. The data collection was done using a National Instruments DAQ, the software LabView, two pressure transducers and a laser displacement sensor. The Version 1 test stand attached to the front of the tool and allowed the user to fire the tool in different orientations. The Version 2 test stand was a mount for the tool – reducing vibration and fixing tool orientation.

4.1.1 Version 1 Test Stand:

Figure 4. Version 1 of the experimental test stand

The initial test stand (seen in Figure 4) was designed to obtain displacement and pressure data. It consisted of a 15” cantilever beam attached to the front of the tool with the displacement sensor mounted at the end of it. This testing setup was susceptible to vibrations which frequently produced inaccurate laser displacement sensor data. Additionally, different tool orientations provided different displacement results, prompting the desire to use a rigid testing mount rather than an attachment.

4.1.2 Version 2 Test Stand:

The Version 2 test stand is shown in Figures 7 (CAD) and 8 (photograph). The test stand is made from 80-20 aluminum because it provides stability as well as ease of manufacturing. The aluminum rails were assembled into a cage around the tool and fastened to the tool using custom made mounts. The tool is fastened to one side of the cage and the laser displacement sensor is fastened to the opposite end of the cage such that the range of the piston’s motion can be recorded with the sensor. This test stand is capable of providing clean, repeatable results with a relatively easy alignment process. Additionally, the cage provides is increased stability which allows for high speed photography of the tool. Data obtained without the cage had a lot of error in displacement due to the violent nature of the

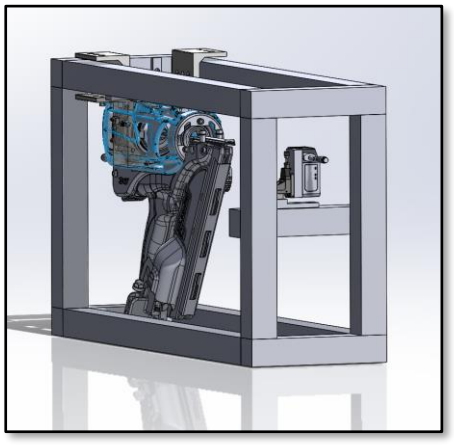

Figure 5. CAD model of test stand.

piston striking the bumper. The cage is secured to the table and vibration is minimized, providing much better results.

The experimental test stand is capable of recording three unique measurements at once. It is equipped with two pressure transducers – one capable of reading pressures up to 300psi and one capable of reading pressures up to 75psi. The 300psi transducer is mounted using a tapped hole through the wall of the combustion chamber. It measures the pressure in the cylinder due to combustion and expansion of volume. The 75psi transducer is mounted to the tool using a tapped hole on the other side of the piston. It records data of pressure due to the piston compressing the second chamber before exhaust air can vent. The pressure in the second chamber is only accurate until the piston passes the port connecting the transducer. Back pressure is a key aspect of the tool because it hinders performance of nail energy but aids in returning the piston to top dead center. One potential issue with this setup is the potential change in performance caused by drilling and tapping holes in the combustion chamber and piston cylinder. This is assumed to be negligible because the transducers were fitted with o-rings and the chamber is not perfectly sealed in ITW's design. Finally, the test stand is equipped with a laser displacement sensor purchased from Keyence. This sensor shoots a laser dot and can record the distance within a range. The sensor and test stand were purchased and designed such that at any point in the piston's travel down the cylinder, the laser would be able to track the piston location. The stand is designed such that the laser is focused on the tip of the piston and it remains on the tip of the piston for the extent of the stroke. Some error still occurs due to misalignment or vibration, but this test stand does a good job of providing accurate displacement data to be compared to simultaneous pressure data.

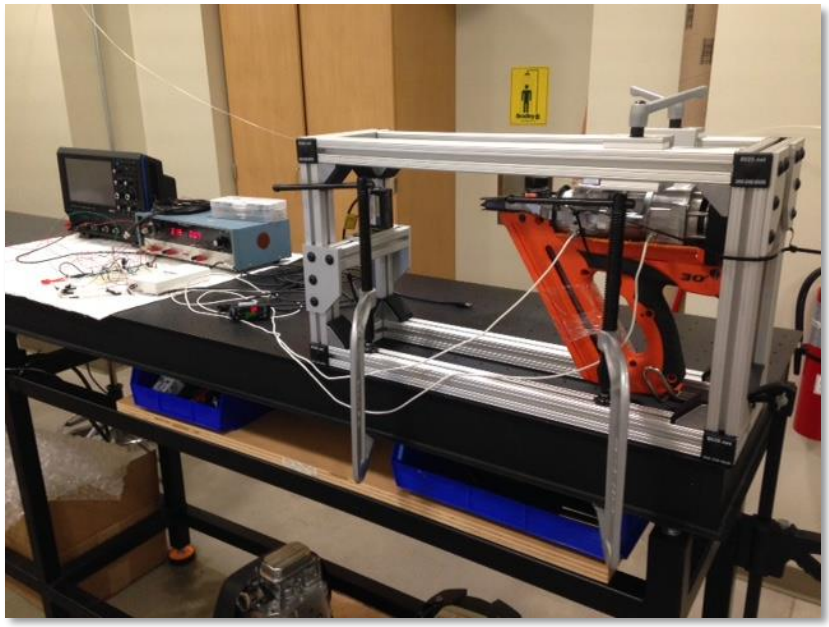

Figure 6. Photograph of new experimental test stand.

The main disadvantage of the laser displacement sensor is the inability to fire nails using the tool. If nails were to be fired, they would be projectiles traveling rapidly towards the expensive sensor. Therefore, a majority of the testing done on the tool was performed by dry-firing the tool. This can change the dynamics of the tool, but because this project focuses on the combustion rise phase, it is assumed that dry-firing the tool gives the research team a solid understanding of how each fuel effects tool performance.

4.2 Flame Visualization

A new combustion chamber was designed with transparent polycarbonate windows on the sides to allow flame visualization. The combustion chamber was machined by Proto Labs using CNC machining. The inner geometry is comparable to the current tool geometry, but with a modest increase in volume (14%). Creating a chamber of similar

geometry is essential to mimic combustion behavior – especially wall extinction of the flame. A key issue that arises with the new combustion chamber is the change in equivalence ratio of the ITW blend. The current fuel dosage of approximately 25mg combined with the original chamber creates an equivalence ratio of 1.04, which is slightly rich. However, the new chamber has more volume and therefore the equivalence ratio is 0.98. This change from rich to lean should be considered when analyzing the results from the dosing of the ITW blend. The new chamber seals around the piston cylinder on one side using sealing rings (Figure 9a). The other side is connected to the sealing element used on the original tool with a custom-made gasket and four bolts (Figure 9b).

Figure 7. Photographs of the mounted, optically-accessible combustion chamber. (a, left) Depiction of the new chamber sealing with the current piston cylinder. (b, right) Depiction of the bolted connection between the original tool sealing component and the new chamber.

The windows provide 1.25” x 1.375” (= 1.72 in^2) viewport into the chamber. The windows are designed to withstand 200 psi of constant pressure with only two bolts

attached. Each window is attached with four bolts to increase the factor of safety and to ensure sealing. A groove was machined into each window and a custom silicone gasket was made to seal the windows. Each window is removeable for the purposes of cleaning or replacement.

The new chamber has four tapped holes in the top to connect to sliding mounts on the aluminum testing rig. The current dosing system requires the tool to be pressed against a surface. Pressing the safety mechanism against a surface serves three purposes: closing the chamber, dosing the fuel, and releasing the lock which prevents the trigger from being pulled. For the laser displacement sensor to track piston location, a new system needed to be devised so the surface would not block the laser line of sight. The sliding mounts can be pushed back to dose the chamber and then locked into place using the set screw handles on the mount. The locks on the sliding mounts also keep the chamber closed at high pressures.

The new chamber creates the ability to take high speed video of the flame propagating through the chamber. The clear windows allow the camera to capture the flame consuming the unburned gas and its interaction with the fan.

4.3 Fuel Comparisons

This study focused on five new fuels with ITW's original blend as the control. ITW blend of fuel consisted of 70% propylene and 30% 1-butene on a molar basis. Fuels were selected based on their lower heating values and flame speeds at stoichiometric conditions. The list of fuels that were tested and their properties can be found in Table 2. Propyne was selected because of its high laminar flame speed. Propane was selected

because of its high LHV. 1-butene, with higher flame speed but lower heating value, served as a compliment to propane to aid in metric testing. Additionally, heptane and iso-octane were selected to be tested. These fuels have lower flame speed than the gaseous fuels tested, but their high volumetric energy density made them appealing options. Iso-octane was also investigated due to its similar ignition behavior to gasoline – a cheap and readily available fuel.

Table 2. Fuel property comparisons (Law, 1998)

	LHV (kJ/g)	S_l at stoich (cm/s)	P_{sat} at 25^0C (psi)	Liquid Density at P_{sat} (kg/m^3)	Vol. Energy Density (kJ/m^3)
1-Butene	45.33	41.74	43.9	625.6	28.36
Propane	46.36	38.65	138.3	580.9	26.93
Propyne	46.17	57.04	83.3	674.4	24.47
ITW Blend	45.66	40.49	131.8	615.6	28.11
Heptane	44.57	38.9	0.8	684.0	30.49
Iso-Octane	44.15	35.0	0.8	690.0	30.46

4.4 Fuel Dosing

The dosing mechanism used by ITW could only be used on the ITW blend. Two new dosing techniques were made to test the fuels from Table 2. The three gaseous fuels are tested with a different technique than the liquid fuels.

4.4.1 Gaseous Dosing:

The gaseous fuels were tested at equivalence ratios between 0.64 to 1.45. Fuel charges for the tool were prepared using a fueling manifold with a 25 mL syringe. This manifold is illustrated in Figure 8. The manifold is vacuumed to ensure the syringe is filled with pure fuel. The syringe was filled to a predetermined volume to obtain a given fuel mass. The syringe is filled to 1 – 2 psig and pressure in the syringe is reduced to atmospheric once detached from the manifold. Once detached from the manifold, any additional mass in the syringe (due to the increased pressure) is expunged and the syringe will contain a pure component at atmospheric conditions (neglecting diffusion from the orifice). Once filled, the syringe is attached to the 1/8" diameter tube connected to the combustion chamber (seen in Figure 9). The combustion chamber is subsequently sealed, so the fuel can be dosed for testing. Sample results illustrating how the combustion chamber pressure change with fuel dosage appear in Figure 10.

The syringe dosing did not come without error in metering. The syringes used had 1 mL tick marks which gives an error of a half of a milliliter. The equivalence ratio is highly susceptible to change if the error is this high so many tests were performed at each condition. Additionally, sealing the chamber causes another issue faced by the tool in everyday use. If the tool were to seal completely, it would be susceptible to locking up. The chamber opens and closes around the piston cylinder. Because of high temperatures, the metal cylinder expands and the chamber hole shrinks. If the fit is too tight, the chamber will not be able to be opened and closed rapidly. Therefore, the seal is made using piston rings. These seals help maintain high pressures, but they are not perfect. When designing the new combustion chamber, a similar fit and seal was designed. Discrepancies in measurements can be a result of varying degrees of successful sealing. Between each fire,

the tool is adjusted for alignment. Any adjustment made has potential to change the degree of sealing success.

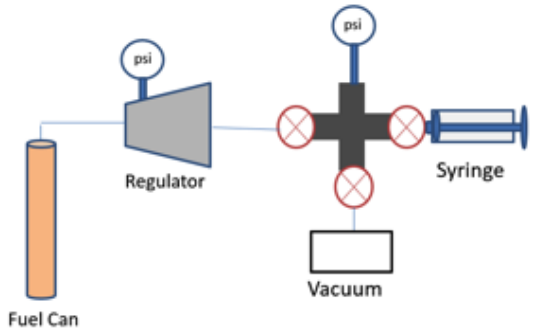

Figure 8. Schematic of the fueling manifold.

Figure 9. (a, left) Dosing syringe attached to combustion chamber. (b, right) “Close up” view of the connection syringe-to-tool connection.

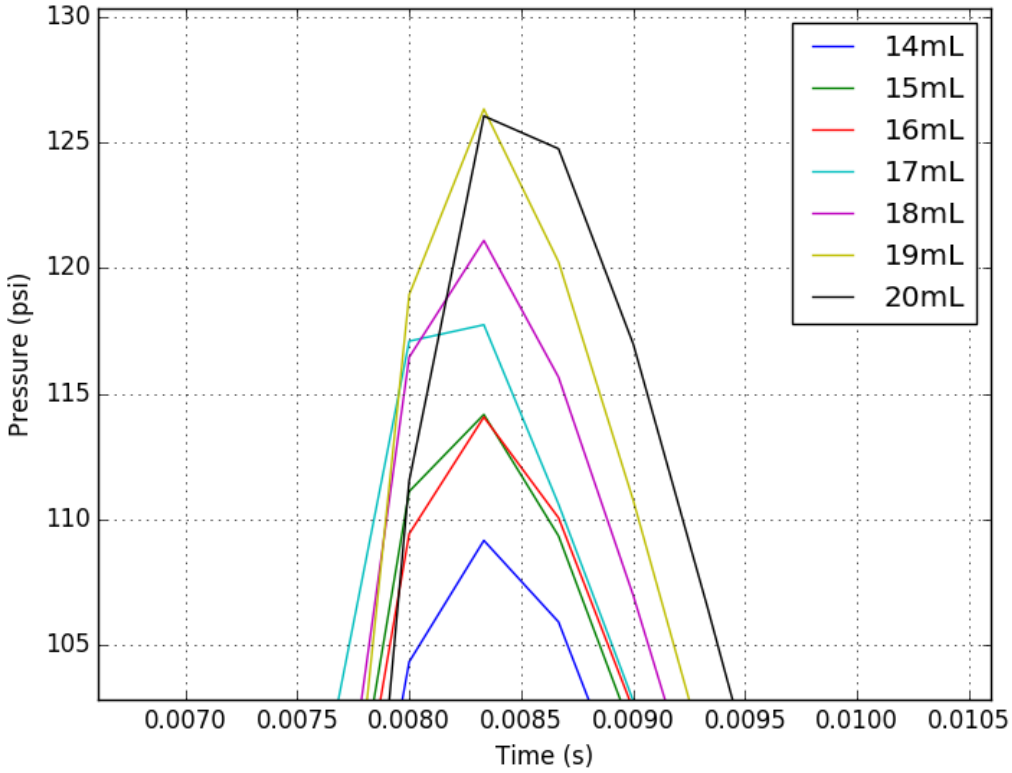

Figure 10. Example of peak pressure profiles for propyne over a range of gaseous volumes dosed into the chamber by the syringe.

4.4.2 Liquid Dosing:

Liquid fuels typically have a much higher volumetric energy density. This is desirable because a dense fuel will provide more shots per cartridge. In order to fire the chamber with liquid fuel, a method of dosing needed to be determined. Dosing gaseous fuels was simple because the fan was able to ensure the blend would be well mixed. Liquid fuels provided a different challenge. For a well-mixed chamber, the liquid needed to be properly atomized, else the tool would not fire. Additionally, regulating the amount of fuel to be dosed was challenging due to the atomization issue. A piston accumulator was designed to pressurize the fuel (Figure 11).

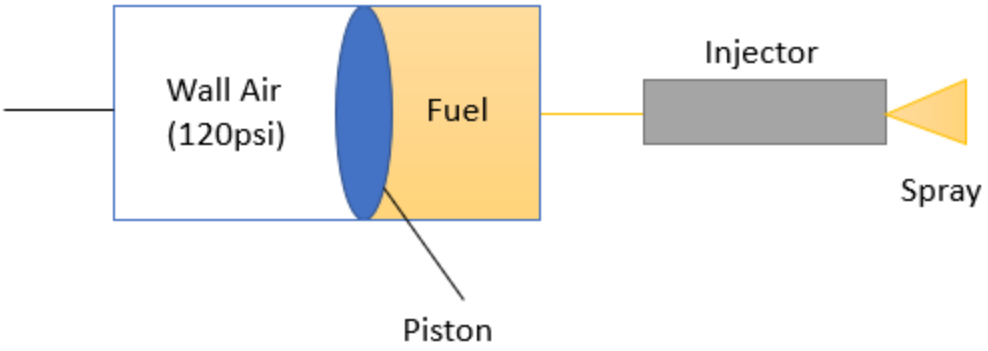

Figure 11. Liquid injection system

The accumulator holds and pressurizes the fuel using a sealed piston. The accumulator is fed compressed air from the wall at 120 psi (seen in Figure 12). The injector is run using a software called CalView. The pulse duration and number of pulses can be varied to determine the amount of mass injected. The injector was calibrated for heptane using a scale that reads variations up to 0.1 mg. The injector provided a range of values to span the chamber's equivalence ratio from 0.77 to 1.07. This was deemed appropriate to test heptane to determine its performance in lean, stoichiometric, and rich conditions. The injector was attached via a ¼" NPT threaded hole tapped into the side of the combustion chamber. The injected mass was atomized due to the small injection port of the fuel injector. The injection was a series of small doses calibrated to match the desired mass and equivalence ratio. It was mixed in the chamber with the fan and then ignited with the spark plug just like gaseous fuels.

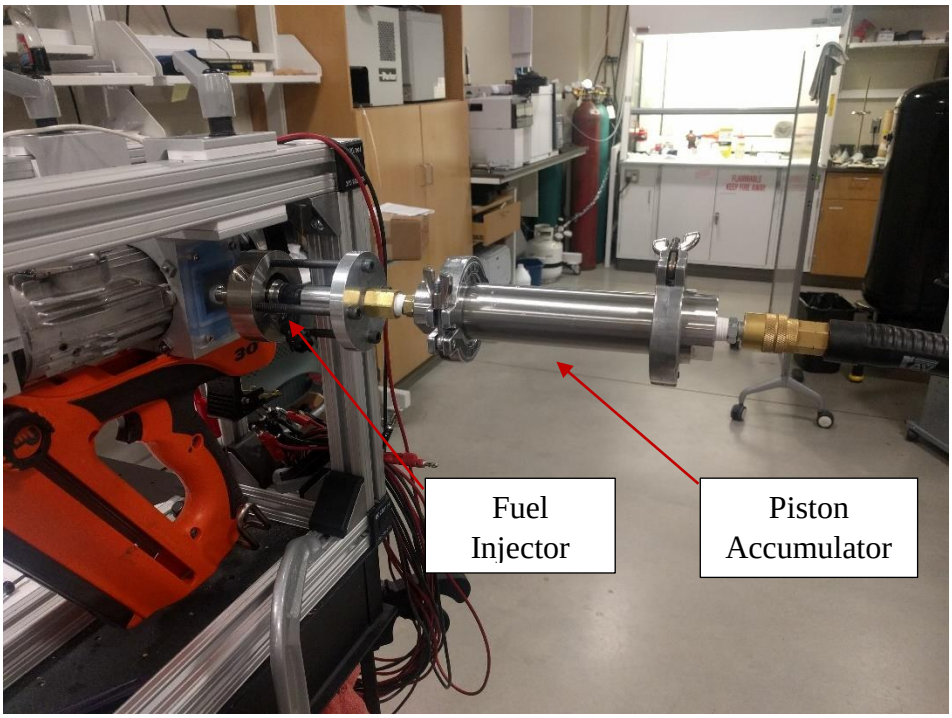

Figure 12. Photo of the accumulator and fuel injector system attached to the tool

Chapter 5. Results

5.1 Experimental Results

Testing was done on the six total fuels at varying conditions. The results of this testing can be found in this section.

5.1.1 Version 1 Test Stand:

Data from the version 1 setup appears in Figure 13, where several “error conditions” are evident in the top pane of the figure. An error occurs during the test when the laser becomes misaligned with the tip of the piston blade – often due to misalignment or vibration. Before plotting, a filter was applied to the data, but the presence of these errors is evident from step-like changes in the data rather than a smooth profile. To obtain a more

accurate depiction of the piston displacement profile, several tests were performed and the ensemble average was taken to smooth out the influence of these errors. This averaged profile is plotted in Figure 13 as a bold red line, along with the raw profiles used for its calculation.

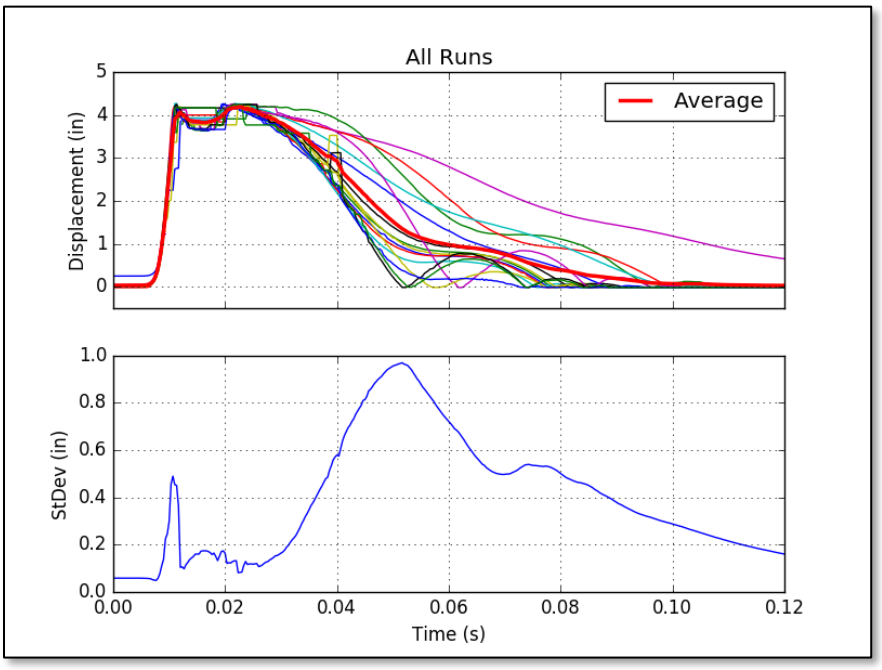

Figure 13. Summary of piston displacement measurements for several runs and the associated ensemble average and standard deviation using the original test setup.

Although these averaged runs give a reasonable depiction of the piston dynamics, ensemble averages can hide important effects (*e.g.*, bumper compression). They can also be difficult to model because they don't represent a single physical run with known boundary/initial conditions. Two of the design goals for the new test stand were (1) to provide a sturdy mounting enclosure that would allow rigid fixing of the tool and (2) to provide a mechanism for fine alignment of the laser sensor. These goals were met through

use of the 80-20 frame and ultimately resulted in better data that eliminated the need for the ensemble average.

5.1.2 Version 2 Test Stand:

Data from a single run with the current 80-20 test stand is reported in Figure 14. The piston displacement data is smooth, showing no obvious discontinuities due to error conditions. In this run, there were 3 error conditions that occurred, but they were short-lived, and are virtually imperceptible in the final data. The data exhibit no errors during the period where displacement is greater than 3 inches, thus the data can be used to characterize bumper dynamics (the bumper is 4.1” away from top dead center). Data with similar quality can routinely be obtained with the new test stand so accurate nail energy calculations can be made and referenced with the pressure that evolves in the chambers. The newer test stand had the capability to provide very accurate results which are essential to obtaining validation results.

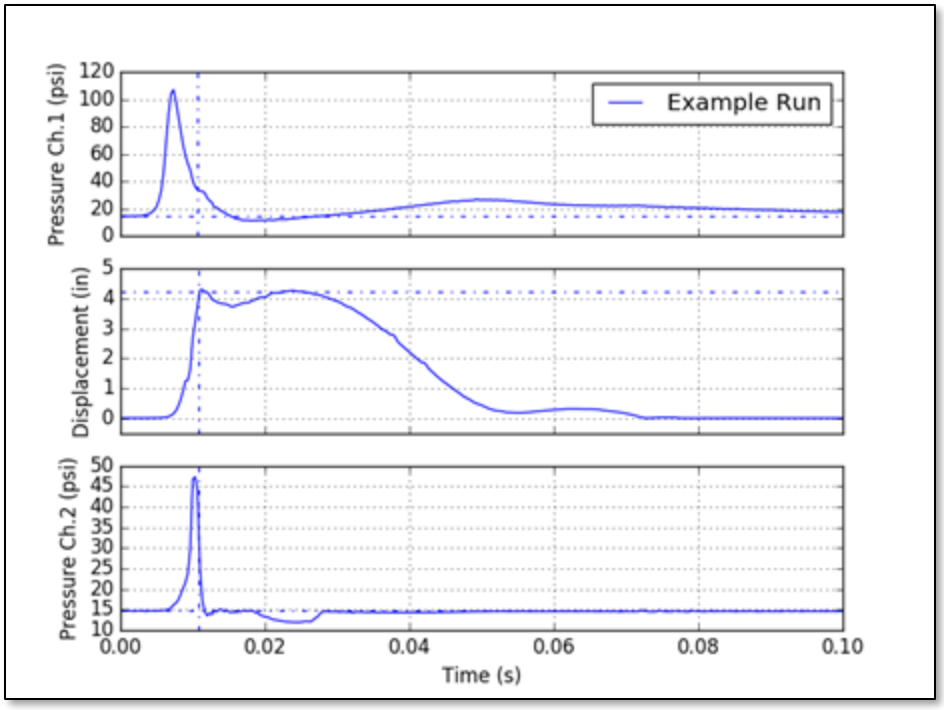

Figure 14. Sample test data from a single run with the second (current) test stand.

Figure 15 shows a plot of the gaseous fuels tested using the Version 2 test stand. This is an average of the six runs at each condition. When peak pressure is investigated, propyne out performs ITW's current blend and 1-butene and propane do not produce the same improvement. Average peak pressure is one option to analyze data, but the next section discusses whether or not Figure 15 is an appropriate method to analyze data.

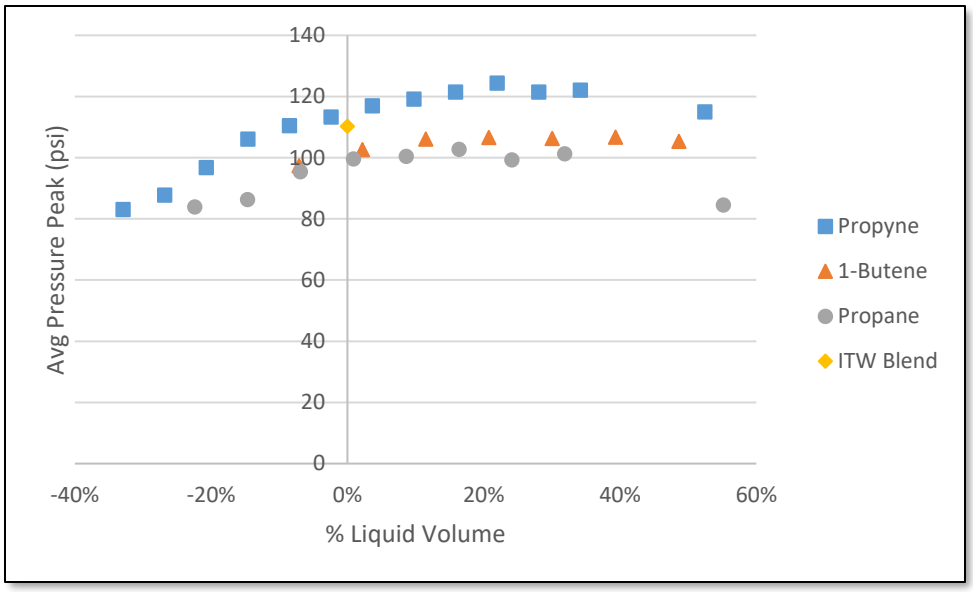

Figure 15. Peak combustion chamber pressure average as a function of percent of liquid volume change

5.1.3 Metric Analysis:

ITW uses nail energy to determine how the tool performs. This is a metric based on the speed which the nail travels. For this project, much of the testing involved the dry-firing of the tool – meaning no nail was fired. It is important to determine a metric which can be used for comparing the tool performance of different fuels. The two metrics analyzed in this section are peak Chamber 1 pressure and boundary work done on the piston.

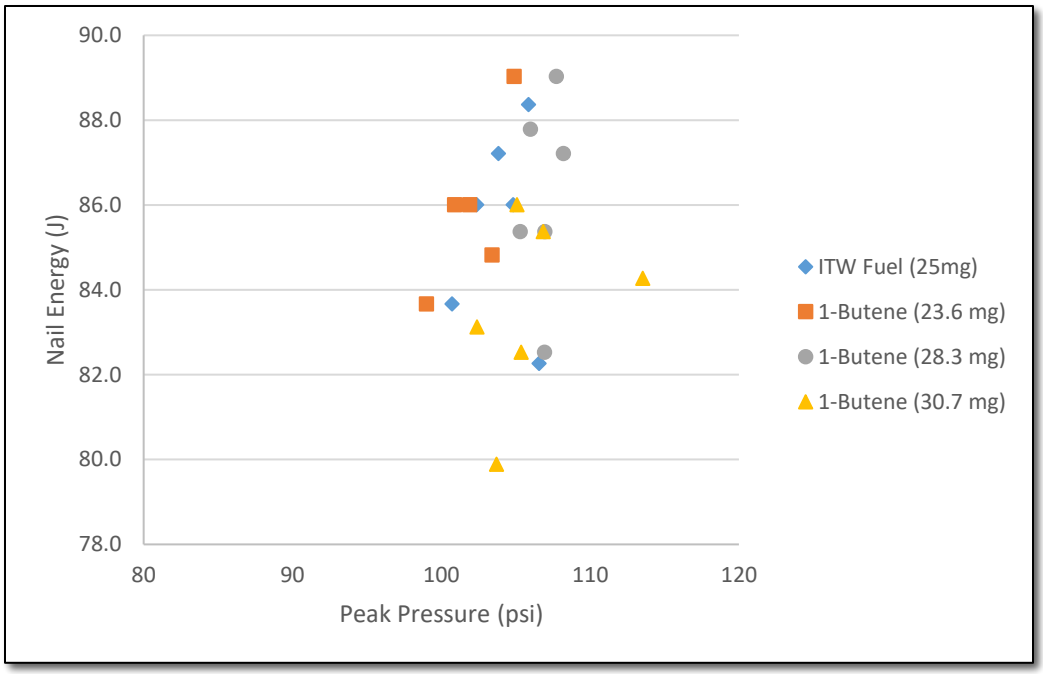

Figure 16. Metric comparison between peak pressure and ITW's nail energy metric

In order to determine whether peak pressure would be an appropriate metric, tests were performed at ITW. Figure 16 is the only data present in the paper where nails were fired from the tool. ITW has a magnetic inductance machine that they use to determine the nail energy from a number of their tools. To operate it, one must fire a nail as a projectile down a horizontal cylinder. The nail travels down the cylinder (without contacting the metal walls) and through a magnetic field. The nail moving through the magnetic field causes a current in the wires wrapped around the cylinder and the time of the pulse (small current) is recorded. The distance between the two coils of wires is a known value and the time it took the nail to pass between the coils is recorded. The nail energy is calculated with the following equation:

Equation 16. Nail energy calculation

$$KE = \frac{1}{2}\, m_{tot}\, v_{nail}^2$$

where KE is the nail energy, m is the mass sum of the piston and the fired nail, and v is the velocity of the nail found using the induction machine. The velocity of the fired nail is a function of a (constant) displacement, or distance between the metal coils, over time between the pulses. Figure 16 shows the results of various fuels tested with the magnetic inductance machine. Due to the nature of how displacement curves are obtained, it is impossible to record simultaneous data for nail energy and work done on the piston without changing methodology.

Overall, there was no strong correlation between nail energy and peak pressure. For each set of points, there is a weak correlation between time and peak pressure. The lack of an overall trend points to the importance of the pressure profile rather than the pressure peak. Each curve has a unique profile with many variables not captured by the peak pressure. Peak pressure does not fully describe how slowly the pressure began rise was or how wide the pressure profile is. Peak pressure is a simple metric which cannot be used to predict higher nail energies within a set of fuels at a given condition/equivalence ratio because it does not capture the full pressure profile. It is important to note that errors were present in these tests – dosing could have been slightly inconsistent, sealing could have caused variation, and the magnetic inductance machine had some approximations for peak locations.

The second metric investigated was the boundary work generated by each fuel. The boundary work done on the piston for each run was calculated by integrating the PdV curve and used as a performance metric for comparing the fuels. Boundary work is the energy produced by a force (pressure acting on the surface area of the piston) acting over a displacement (the firing stroke of the piston). This metric to evaluate tool performance

should be identical to nail energy if heat loss, frictional forces, and losses due to nail collision were neglected.

The correlation between boundary work and peak nail energy would be strong if it were not for one factor – the fan. The impact of the fan is central to the turbulent combustion in the chamber. To determine the significance that the fan turbulence had on flame propagation, testing was done on the tool with the fan blade removed from the chamber. Six tests for each fuel were run at stoichiometric conditions and the data sets were recorded. Additionally, to ensure the fuel was completely mixed, the tool was fired one, two, and five minutes after a unique dose – minimal leakage occurred in this set of tests. No set of times between dosing and firing proved to be optimal. These well mixed conditions provided the same results as the tests run without additional mixing time. Figure 17 shows the comparison between individual runs of the "No Fan" condition (depicted NF) and individual runs of the "Fan" condition.

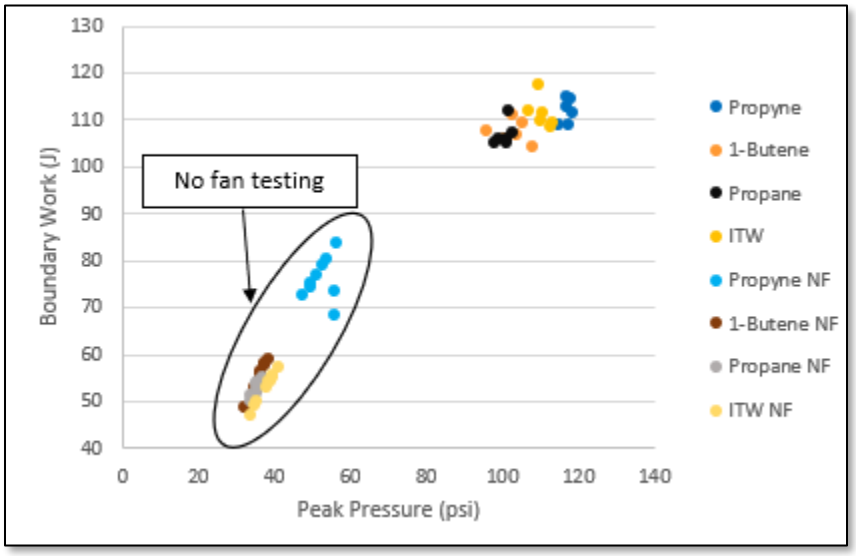

Figure 17. Boundary work vs peak pressure – NF indicates no fan

The fan creates a higher work production and a higher peak pressure, but it also creates more chaos in results. Without the fan, the correlation between peak pressure and boundary work is linear and flame speed is a more important parameter for the fuel (propyne has the highest flame speed by at least 15 cm/s). Once the fan is added at the same stoichiometry, the comparison no longer linear. The fan negates the significance of the laminar flame speed. Propyne still has the highest peak pressures with the fan, but the positive linear correlation between peak pressure and PdV is lost.

Without the fan, there is a strong positive correlation between peak pressure and boundary work, but the acceleration of the flame propagation due to the fan-produced turbulence ruins this correlation. For this thesis, boundary work is the metric that is used to analyze tool performance.

5.1.4 Boundary Work

Six tests at varying equivalence ratios (determined by volume of gaseous fuel in the syringe) were performed for the three fuels. Additionally, the current blend was tested as a control. The calculated boundary work is compared for each fuel in Figure 18, where it is plotted as a function of liquid volume reduction relative to the current blend (*i.e.*, how much less volume on a percentage basis is required for a nail gun test relative to the current blend to achieve the same amount of work).

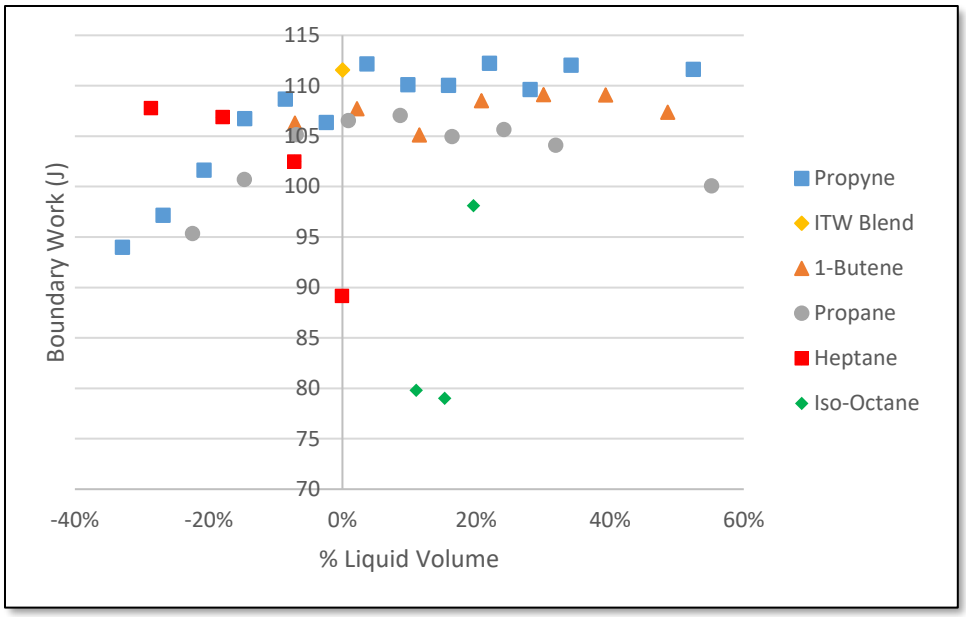

Figure 18. Average boundary work on the piston as a function of percent of liquid volume change.

While none of the candidate fuels outperform the current blend in this metric, there is much to be taken from these data. With an 8% reduction in liquid volume, propyne was able to provide results within 5% of the original blend. Once the doses are made richer, many of the fuels can produce similar (within 5%) or slightly better results than the current blend, on average. The variance in testing for these conditions is high, which can be attributed to two factors: 1) the measurement errors of the syringe or errors caused by fuel being left in the tubing attaching the dosing manifold and the chamber (see Figure 9b) and 2) the inconsistent sealing of the combustion chamber causing pressure leakage. Investigating mean performance shows it is possible to produce similar nail energy using a different fuel.

The liquid fuels that were tested were heptane and iso-octane. Heptane was the better of the two liquid fuels tested – providing strong performance at a reduction of liquid volume. Iso-octane did not perform well, but this is in part due to errors in calibration and

small sample size. The low boundary work and increased liquid volume is likely a result of inconsistent dosing. These two fuels were chosen because they have high energy densities compared to the gaseous fuels tested before them. Both fuels have a low laminar flame speed at stoichiometric conditions, iso-octane at 35 cm/s and heptane at 38.9 cm/s. The fuels also have a lower LHV than the gaseous fuels. These fuels are made of heavier molecules and provided a greater volumetric energy density. Some issues did arise when testing these fuels, most notably the atomization of the molecules. Initial tests of these liquids would not fire due to the fuels remaining in liquid form. This caused the fuel-air mixture to be too lean to ignite when sparked. Once the high-pressure injector was put into operation, much of this problem was resolved.

Testing was performed on heptane for two lean conditions, a stoichiometric condition, and a rich condition. The tops of the pressure profiles can be seen in Figure 19. The discrepancies between same mass runs can be attributed to inconsistent chamber sealing or dosing errors. Heptane demonstrated the ability to produce pressure comparable to 1-butene and propane at a significant decrease in volume. 1-Butene's peak pressure came near stoichiometric conditions and was two psi greater than heptane's stoichiometric peak. Overall, heptane would be a better replacement than pure 1-butene or propane because it is denser in liquid form and outperforms (propane) or matches (1-butene) in the boundary work metric. Heptane would be a desirable substitute because of its density but there would likely be a decrease in nail energy compared to the current blend or compared to propyne. Heptane should be considered as a blend substitute to 1-butene because it is denser in liquid form and provides the same results.

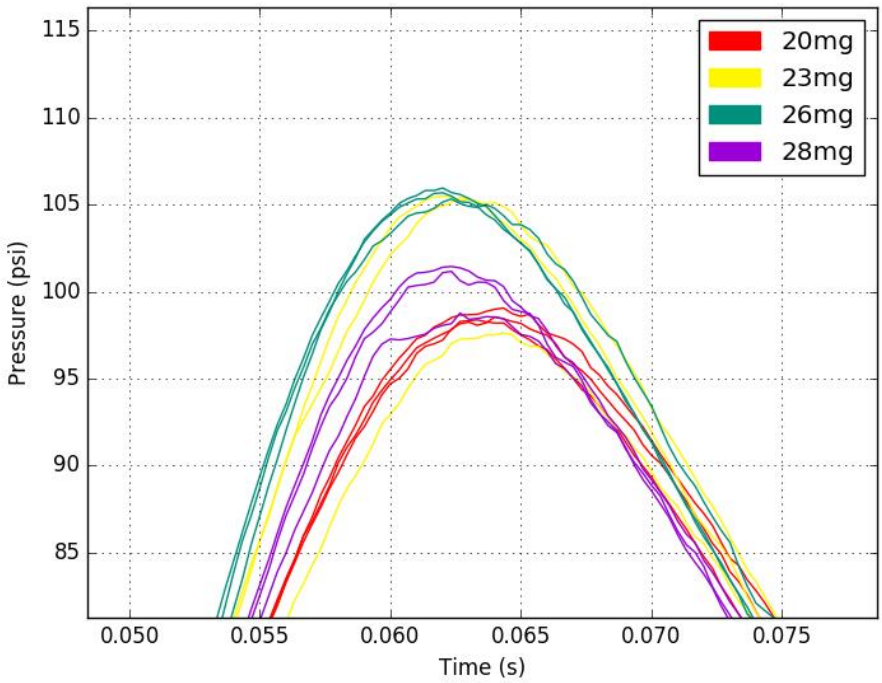

Figure 19. Pressure profiles near peak for liquid heptane

Iso-octane requires more testing to provide conclusive results – this is partially due to issues with dosing. The larger molecule provided a difficult time for calibration, testing, and tool firing. When data were recorded, it was unknown at which equivalence ratio the data were recorded. During calibration, the same settings in CalView provided significantly different masses each time they were run. This could be caused by sensor error, wall pressure inconsistency, or due to rapid evaporation of iso-octane. The peak pressures of iso-octane were lower than those of propane – this makes sense because the LHV and flame speed at stoichiometric conditions were also lower. Iso-octane could be an ideal substitute fuel because of its liquid density. It has the highest liquid density of the fuels tested but the performance does not merit using it as a replacement fuel. Iso-octane was tested in part due to its similarities to gasoline. While iso-octane is a pure substance, gasoline is a blend of fuels that is readily available and more cost effective. Unfortunately, when gasoline was

tested in the tool, the tool would not fire. This is likely due to atomization issues similar to those that arose when testing iso-octane. Gasoline is a blend of fuels with even heavier compounds than iso-octane and heptane. Gasoline also has many lighter compounds which also caused some calibration issues. Mixing this blend with air requires more effort than heptane and iso-octane did.

The liquid fuels tested provided a drop-off in performance. This was anticipated due to the LHV and flame speed of the fuels. They do, however, provide the most value for volumetric energy density, as seen in Table 2. A goal ITW has for their tool is to reduce the number of times users need to change the cartridge. If a fuel can generate more power per cannister, or set volume, it is a more appealing fuel. The drop off in performance is mitigated by the increase in shots per cartridge for liquid fuels.

Table 3 shows an analysis of peak boundary work and the number of shots per cartridge for each fuel. The shots per cartridge numbers are approximations based on saturation pressure density and stoichiometric conditions. The peak boundary work data points were taken from tests run near stoichiometric conditions (some slightly leaner, some slightly richer). If peak boundary work is the key performance indicator, propyne slightly outperforms the current blend. However, at stoichiometric conditions, propyne performs very poorly in the shots per cartridge column. It is important to have a balance between high boundary work produced and volumetric energy density so that one can maximize the shots per cartridge in the system. A blend of propyne (pressurized to be in liquid form) and heptane would be an interesting option for ITW to attempt because there is the possibility

to achieve both the increase of shots per cartridge and increase of shot power with the correct blend.

Table 3. Fuel comparison based on peak boundary work

	Avg. Peak Boundary Work (J)	Mass Required for Stoich. (mg)	Number of shots (based on ITW = 1200 shots)
1-Butene	109	24	1219
Propane	107	22.6	1203
Propyne	113	25.7	965
ITW Blend	112	24	1200
Heptane	108	23.3	1373
Iso-Octane	98	24	1345

5.1.5 Fuel Blending (Gases):

Using two dosing manifolds (seen in Figure 8) hooked up to two different fuel canisters, the syringe can be easily detached and reattached to the Luer-lock connector. The fuels can be filled into the same syringe and dosed into the chamber using the same method for testing pure fuels. The syringe was filled with the appropriate volumes of propane and propyne and dosed into the chamber for a stoichiometric condition. To see if order of filling made a significant impact on the dosing, two different trials were performed – the syringe was filled propane first then propyne for the first trial and the order was flipped for the second trial. According to Figure 20, there is no evidence that the order has an impact. The figure also shows that a 50/50 molar blend at the same stoichiometry produces a 50/50 blend between the boundary work and the peak pressure. The linear pattern seen in the no fan testing remains the same.

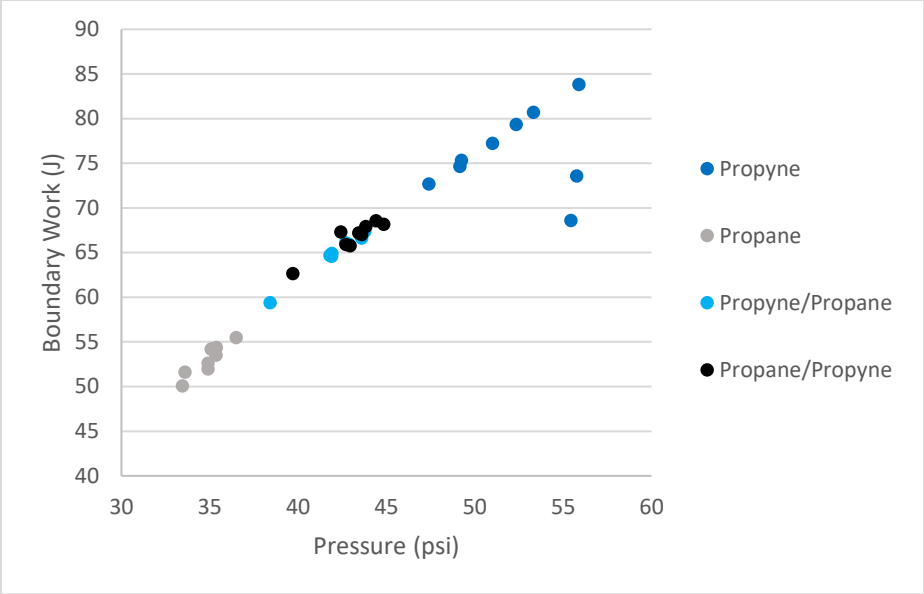

Figure 20. Blend analysis between propane and propyne without the fan blades

5.2 Comparison with model predictions

The ITW blend of 70% propylene and 30% 1-butene was compared to the model predictions. The model was able to aid in selecting candidate fuels but it requires more sophisticated sub-systems to properly predict tool performance.

5.2.1 Experiment and model comparison:

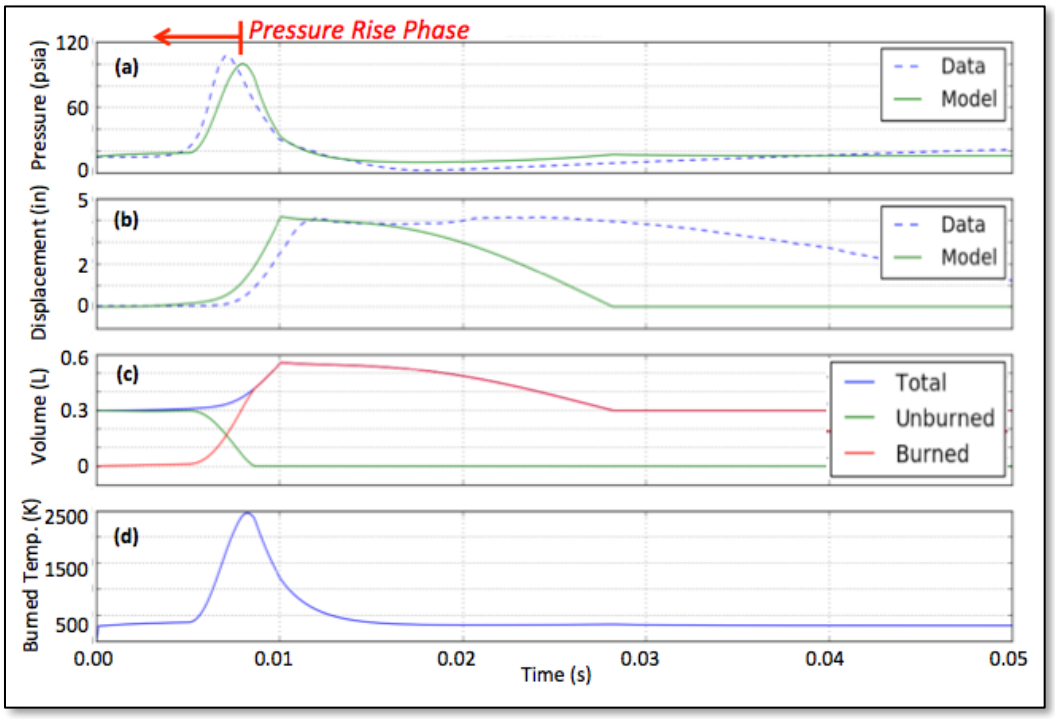

Figure 21. Comparison of bi-zonal model results with data.

Sample results from the model are shown in Figure 21. Parts (a) and (b) compare the pressure and piston displacement predictions, respectively, with experimental data. The qualitative agreement between the model and data is satisfactory, but improvements are needed in the quantitative accuracy. Once the flame propagation has been fully characterized, the results/insight can be used to improve the accuracy of the model during the pressure rise phase (denoted in Figure 21a). Accurate predictions during that period are especially important for this project as they govern the nail energy. Figure 3b is an example of discrepancy between the displacement data recorded and the model. The model shows a slower pressure rise time (21a) but an earlier piston stroke (21b) than the actual data. This is due to the inaccuracies in the modeling of Chamber 2 pressure and friction. Figure 21c shows model predictions of the volume in the tool, and how it

transitions from unburned to burned gas as the flame propagates through the mixture. The influence of changing volume is also evident in this subplot, as the total volume initially increases before returning to the initial volume upon piston return. Figure 21d plots the burned temperature calculations during the simulation. The burned gas temperature approaches the adiabatic flame temperature for this configuration, and then quickly decays due to the expansion of the gas.

5.2.2 Flame Front Visualization:

With the current setup, photography was digitally recorded using a Photron Fastcam APX RS high-speed digital camera. In Figure 22a, the flame can be seen almost completely filling the combustion chamber. Figure 22b shows a millisecond later - the luminous intensity is empirically greater, and the entire chamber looks to be in flames. One issue with the visual inspection is that it was difficult to determine what is flame and what is visible radiation due to hot gases. Due to this ambiguity, only a range of burn duration can be determined. Based on visual inspection of three runs with the ITW fuel, burn duration was determined to be between 5 and 8 milliseconds. This is an important finding because it created an appropriate range for the flame speed wrinkling factor. This is one example of how experiments can reduce the number of unknowns in the model.

Figure 22. Flame visualization (a, left) 0.5 milliseconds before peak pressure and (b, right) 0.5 milliseconds after peak pressure. The red line on the left depicts the flame front.

Another important aspect determined by the flame visualization was the turbulent nature of the flame. The flame surface area was modeled before flame visualization as a radially propagating hemisphere and turbulence was accounted for as a multiplier to laminar flame speed, causing the hemisphere to grow faster. The high-speed video shows that this assumption is not valid, and it is a source for error within the model. Once the other sub-systems in the model are validated, a more robust turbulent flame propagation model should be developed.

Chapter 6. Summary and Future Work

6.1 Summary

Experiments were done on the XP Framing Nailer to determine how different fuels affected tool performance. Volumetric energy density was the most important fuel characteristic for tool performance. Flame speed ended up being a deciding factor for obtaining peak pressure in the chamber, but it did not maximize the performance of the tool. ITW sought a more powerful fuel as well as a fuel that could provide more shots per

cartridge. Fuels with higher volumetric energy density would provide more shots per cartridge (assuming a constant volume fuel cannister).

Additionally, a physics-based model was created to investigate the framing nailer. The model had limitations, but it was able to predict the importance of flame speed and the lower heating values with regards to fuel selection. Testing was performed to validate the model and determine what characteristics of fuels were desirable to optimize tool performance.

The project provided results upon which to build and a model with a solid foundation. The most promising results produced were propyne's performance as well as the adequate performance of liquid heptane. Both fuels would be good candidates for further testing and possible integration into ITW's fuel offerings.

6.2 Future Work

6.2.1 Modeling Work:

The modeling portion of the project requires a lot of future work. Initially, the model was designed to predict fuels that would perform best within the tool. Experimentation was designed only for model validation. The model ran into road bumps developing the physics of the tool. The XP nailer is a complex tool with a lot of dynamics happening inside of it. It became difficult to focus on the combustion side of the tool without first settling question marks in the submodels such as friction, compression in the back chamber, bumper dynamics, the addition of heat loss, and nail effects. The key combustion improvement to the model is determining an accurate model for turbulent flame propagation. The fan inside of the chamber was not properly modelled because it

would have been difficult to determine that model's validity. Compounding errors in each sub-model crippled it and made a valuable sub-model useless. Instead of spending time focused on turbulent combustion, the project shifted to a more experimental based procedure with the model informing what experiments should be performed.

The most important sub-model to be fixed would be adding the fan dynamics to the combustion process. With this, the user would gain a better understanding of how the fuels burn rather than approximating the pressure profiles. This may require computational fluid dynamics or a high-level turbulent combustion model appropriated for the Paslode tool.

6.2.2 Experimental Work:

More work should be done on the experiments as well. For a project focused on fuel, a lot of issues with the tool caused the results to skew. Eliminating the variability caused by the tool's dynamics would allow researchers to focus on the combustion aspect of the tool. The chamber's inability to fully seal creates problems analyzing data and the inconsistencies that arise with dosing only enhance that issue. This study would benefit from a redesigned "test" tool with a similar combustion chamber and piston/cylinder setup. If the tool sealed properly and had a consistent dosing method been employed, results would have been much clearer. This could be avoided if testing was done in a separate apparatus created to simulate tool dynamics.

Additionally, the dynamics caused by the fan and the spark plug could prove to be crucial to the performance of the tool. A spark with greater energy could aid in flame propagation and help with tool performance. Additionally, dual spark systems have been shown to aid in reducing burn duration (and therefore increasing chamber pressure). The

fan is another aspect that could be optimized. It runs at a constant of roughly 1000 RPM. If the fan speed was changed such that peak tool performance would be more regular given the fuel conditions, the users enjoy more consistent and effective tool performance. Fan speed and spark energy (and quantity) are two aspects that the paper was unable to analyze.

Determining a correlation between boundary work, peak pressure, nail energy, and any other metric would also benefit the project. The tool performs differently when a nail is being fired vs being dry-fired and it could cause some error in the analysis. Data acquisition while firing a nail would be advantageous for the continuation of this project.

An interesting blend to try for the candidate fuel would be a blend of propyne and heptane. Liquid fuels have the advantage of high volumetric energy density, but they come with low LHV and flame speeds. A fuel like propyne has contrasting benefits. A pairing of the two fuels could provide ITW with a fuel that burns fast and is volumetrically dense – future researchers should test this hypothesis.

Another current solution could be replacing propene with heptane in the current blend. ITW's current blend performs well compared to most fuels tested, but it is 30% 1-butene on a molar basis. Heptane was shown to have similar results with 1-butene but has a higher volumetric energy density. Further testing should be done to confirm these results.

Finally, more testing should be done with more fuels. This project attempted to cover a wide range of fuels – some with high LHV and flame speeds and others with low LHV and flame speeds. More fuels tested could provide more insightful conclusions because more data is available. Additionally, a better method for atomizing/testing liquid fuels is important to gain a better understanding of how fuels like heptane, iso-octane, and gasoline perform. With more results, a stronger conclusion can be determined – helping

ITW, the consumer, and the developer of the model. The current blend is a good source of energy for the tool, but the experiments in this paper demonstrate that fuel optimization is possible.

BIBLIOGRAPHY

About Cantera. (2018). Retrieved from Cantera: https://www.cantera.org/docs/sphinx/html/about.html

Boles, Y. A. (2015). *Thermodynamics: An Engineering Approach.* New York: McGraw-Hill Education.

Christian Foin, K. n. (1999). A diagnostic bi-zonal combustion model for the study of knock in spark-ignition engines. *JSAE Review 20*, 401-406.

Harris, T. (n.d.). *How Nail Guns Work*. Retrieved from howstuffworks: https://home.howstuffworks.com/nail-gun.htm

Heywood, J. B. (1988). *Internal Combustion Engine Fundamentals.* McGraw-Hill Inc.

Koehler, K. (2018, June 25). *Best Framing Nailer Review and Shootout*. Retrieved from Pro Tool Reviews: https://www.protoolreviews.com/tools/air/framing-nailers/pneumatic-full-head-framing-nailer-roundup/9878/3/

Law, S. D. (1998). Laminar Flame Speeds and Oxidation Kinetics of iso-Octane-Air and n-Heptane-Air Flames. *Twenty-Seventh Symposium (International) on Combustion*, (pp. 521-527).

M. Grill, T. B. (2006). Quasi-Dimensional Modeling of Spark Ignition Engine Combustion with Variable Valve Train. *SAE International.* Detroit, Michigan.

Mahoney, D. (2010, August 6). *Cordless Nail Gun Comparison Test*. Retrieved from Popular Mechanics: https://www.popularmechanics.com/home/tools/reviews/a6022/cordless-nail-gun-comparison-test/

MAPP Gas. (2018). Retrieved from Wikipedia: https://en.wikipedia.org/wiki/MAPP_gas

Paslode's New CF325XP & PF250S-PP Nailers. (2015, December 1). Retrieved from Nail Gun Depot: https://www.nailgundepot.com/blog/paslodes-new-cf325xp-pf250spp-nailers-blog.html

S. G. Davis, C. K. (1998). Determination of and Fuel Structure Effects on Laminar Flame Speeds of C1 to C8 Hydrocarbons. *Combustion Science and Technology*, 427-449.

Safety Alert - Safe Use of Nail Guns. (2012, May 22). Retrieved from Safety Concepts: http://safetyconcepts.com.au/safety-alert-safe-use-of-nail-guns/

Sokratis Demesoukas, C. C. (2013, 9 8). Zero-Dimensional Spark Ignition Combustion Modeling - A Comparison of Different Approaches. *SAE International*.

Turns, S. R. (2012). *An Introduction to Combustion: Concepts and Applications.* New York: McGraw-Hill Education.